

Nontrivial effect of dephasing: Enhancement of rectification of spin current in graded XX chains

Saulo H. S. Silva¹,[✉] Gabriel T. Landi,² and Emmanuel Pereira^{1,*}

¹*Departamento de Física, Instituto de Ciências Exatas, Universidade Federal de Minas Gerais, 30123-970, Belo Horizonte, Minas Gerais, Brazil*

²*Instituto de Física da Universidade de São Paulo, 05314-970 São Paulo, Brazil*



(Received 8 July 2022; revised 7 March 2023; accepted 10 April 2023; published 19 May 2023)

In order to reveal mechanisms to control and manipulate spin currents, we perform a detailed investigation of the dephasing effects in the open XX model with a Lindblad dynamics involving global dissipators and thermal baths. Specifically, we consider dephasing noise modeled by current-preserving Lindblad dissipators acting on graded versions of these spin systems, that is, systems in which the magnetic field and/or the spin interaction are growing (decreasing) along the chain. In our analysis, we study the nonequilibrium steady state via the covariance matrix using the Jordan-Wigner approach to compute the spin currents. We find that the interplay between dephasing and graded systems gives rise to a nontrivial behavior: When we have homogeneous magnetic field and graded interactions we have rectification enhancement mechanisms, and when we have fully graded systems we can control the spin current in order to keep the direction of the particle and/or spin flow even with inverted baths. We describe our result in detailed numerical analysis and we see that rectification in this simple model indicates that the phenomenon may generally occur in quantum spin systems.

DOI: [10.1103/PhysRevE.107.054123](https://doi.org/10.1103/PhysRevE.107.054123)

I. INTRODUCTION

Transport in quantum devices has been receiving increasing attention due to the possibility of building smaller systems, which in turn has sharpened our understanding of nonclassical effects on fluxes of energy or particles. The comprehension of these behaviors, precisely, the derivation of transport laws from the underlying microscopic dynamics, is one of the fundamental issues of nonequilibrium statistical physics.

The investigation of transport in low-dimensional systems also deserves attention and raises interesting problems, in both classical and quantum regimes [1–4].

An important and recurrently studied transport property is the existence of rectification, namely, a preferential direction for the flow. Many works are devoted to study what types of interactions the system has to present to guarantee rectification [5–9].

In the quantum regime, open spin quantum systems governed by Lindblad equations have been shown to present rectification and other interesting behaviors with promising applications for the manipulation of the energy and spin flow [10–17,23]. To give an example, we recall studies involving an Ising chain with thermal reservoirs attached to its ends: For a junction with two spins and a longitudinal field, it has been shown that perfect rectification occurs [18]. Considering systems larger than two spins in the Ising chain, in Ref. [19], conditions to keep the perfect rectification are presented. For more complex systems, such as the XX chain, it is observed

in Ref. [20] that the rectification factor does not tend to zero at the thermodynamic limit.

In this context, an interesting problem is the effect of dephasing noise in the quantum transport. In particular, the problem considered in the present paper is of interest for the effect of dephasing in the rectification property.

The role played by dephasing in transport has been investigated, mainly in *boundary-driven* systems. As an example, we cite interesting results described in Refs. [21,22]: For any nonzero dephasing strengths, free tight-binding models typically become diffusive in the thermodynamic limit. In Ref. [23], it is demonstrated that the interplay between dephasing and a particular type of on-site potential, namely quasiperiodic potential, gives rise to an enhancement of transport, increasing the system's conductivity. In Ref. [24], a detailed investigation of the heat flow on an XXZ chain is performed when bulk dephasing takes place, both on the weakly interacting and strongly interacting regimes.

It is important to recall that the XXZ chains are the prototypes for open quantum spin systems. In particular, the rectification phenomena has already been investigated in these models. In Ref. [25], it is shown the absence of spin rectification in the system with zero anisotropy parameter Δ (coefficient of $\sigma_j^z \sigma_{j+1}^z$) and for $\Delta \neq 0$, rectification is observed. It is also well known that the XXZ model can be mapped into another problem: bosons with creation and annihilation operators, with quadratic terms and a quartic term proportional to Δ (Tonks-Girardeau model). The vanishing of rectification in the absence of the quartic term has an analogy with the case of classical oscillators, where it is known that there is no rectification in the absence of anharmonicity (or other effect beyond pure harmonicity).

*emmanuel@fisica.ufmg.br

Motivated by the vast transport properties of open quantum systems and by the interesting effects of dephasing noise on transport, in the present work we perform an analytical and numerical detailed investigation of the XX spin-1/2 model, subject to thermal baths and dephasing noise. Using the global Lindblad master equations, we focus on a specific type of asymmetric systems, the *graded* chains. We remark that graded models have already demonstrated to be precise systems for the occurrence of rectification [26–28]. In the present paper, we show a very interesting and nontrivial effect: The addition of dephasing (which, we recall, means a kind of noise), in some cases, may increase the spin current and also the spin rectification in these graded XX spin models. Our research is, in some way, inspired by the occurrence of considerable changes in the heat current for the classical chain of oscillators due to the presence of noise. Precisely, a chain of harmonic oscillators changes the behavior of the heat transport from ballistic to diffusive (obeying the Fourier law) as we introduce self-consistent stochastic inner reservoirs; see, e.g., Ref. [9].

The rest of the paper is organized as follows. In Sec. II, we introduce the model and some preliminary details about the study of the nonequilibrium steady state (NESS). In Sec. III, we describe the currents and some properties using the covariance matrix. In Sec. IV, we perform numerical results for the spin rectification with dephasing. Section V is devoted to concluding remarks.

II. MODEL AND PRELIMINARY DETAILS

Our model under study is the one-dimensional quantum XX spin chain with N sites, described by the Hamiltonian

$$H = \sum_{j=1}^N \frac{h_j}{2} \sigma_j^z + \frac{1}{2} \sum_{j=1}^{N-1} \alpha_j (\sigma_j^x \sigma_{j+1}^x + \sigma_j^y \sigma_{j+1}^y), \quad (1)$$

where σ_j^j are the usual Pauli matrices, h_j is the external magnetic field acting on site j , and α_j is the exchange interaction between spins j and $j+1$. The rectification and the fluxes present on the system will be directly associated with the asymmetry of the coefficients h_j and α_j with respect to the left-right reflection of the chain.

The system is coupled on the first and last sites to thermal reservoirs, kept at temperatures T_L and T_R , respectively. The thermal baths are modeled by an infinite number of bosonic degrees of freedom given by the Hamiltonian

$$H_E^i = \sum_l \Omega_{i,l} a_{i,l}^\dagger a_{i,l}, \quad (2)$$

where $a_{i,l}$ are a set of independent bosonic operators and $\Omega_{i,l}$ are the corresponding frequencies, which we assume to take on a quasicontinuum of values in the interval $[0, \infty)$. The interaction with the first and last sites is assumed to take the form

$$H_I^L = \sigma_1^x \sum_i g_i (a_{L,i}^\dagger + a_{L,i}), \quad H_I^R = \sigma_N^x \sum_i g_i (a_{R,i}^\dagger + a_{R,i}). \quad (3)$$

In order to proceed with the study of the currents, we recast the problem as a Lindblad master equation in the *weak*

coupling regime [29], where the time evolution of the system's density matrix ρ is given by

$$\frac{d\rho}{dt} = -i[H, \rho] + \mathcal{D}_L + \mathcal{D}_R, \quad (4)$$

where \mathcal{D}_L and \mathcal{D}_R are the Lindblad dissipators associated to the baths. It is possible to derive them from Eq. (3) using the method of eigenoperators [29].

To obtain a better representation of the Hamiltonian, we transform it in terms of σ_l^+ and σ_l^- operators given by

$$\sigma_l^+ = \frac{1}{2}(\sigma_l^x + i\sigma_l^y), \quad \sigma_l^- = \frac{1}{2}(\sigma_l^x - i\sigma_l^y), \quad (5)$$

and then the Hamiltonian in (1) becomes

$$H = \sum_{j=1}^N \frac{h_j}{2} (\sigma_j^+ \sigma_j^- - 1/2) + \frac{1}{2} \sum_{j=1}^{N-1} \alpha_j (\sigma_j^+ \sigma_{j+1}^- + \sigma_j^- \sigma_{j+1}^+). \quad (6)$$

In order to study the dissipators in the Lindblad equation, we must diagonalize H . To do this, we use a fermionic representation through the Jordan-Wigner transformation [30,31] given by

$$\eta_l = Q_l \sigma_l^-, \quad \eta_l^\dagger = Q_l \sigma_l^+, \quad (7)$$

where $Q_l = \prod_{j=1}^{l-1} (-\sigma_j^z)$.

Following this transformation, the Hamiltonian is given by a quadratic form in the fermionic operators

$$H = \sum_{j=1}^N h_j \eta_j^\dagger \eta_j + \sum_{j=1}^{N-1} \alpha_j (\eta_j^\dagger \eta_{j+1} + \eta_{j+1}^\dagger \eta_j) = \sum_{n,m} W_{n,m} \eta_n^\dagger \eta_m, \quad (8)$$

where $W_{n,m}$ is a matrix with entries $W_{j,j} = h_j$ and $W_{j,j+1} = W_{j+1,j} = \alpha_j$.

It is possible to put H in diagonal form; that is, we first diagonalize the matrix W . Since it is symmetric, it may be diagonalized by an orthogonal transformation $S_{n,k}$ ($S^\dagger S = 1$) as

$$W_{n,m} = \sum_{k=1}^N \epsilon_k S_{n,k} S_{m,k}. \quad (9)$$

Here we define a new set of fermionic operators,

$$\tilde{\eta}_j = \sum_{k=1}^N S_{j,k} \eta_k, \quad (10)$$

in terms of which Eq. (9) becomes

$$H = \sum_{k=1}^N \epsilon_k \tilde{\eta}_k^\dagger \tilde{\eta}_k. \quad (11)$$

As derived in a previous work [20], the dissipators are given in terms of this new set of fermionic operators:

$$\begin{aligned} \mathcal{D}_L(\rho) = & \sum_{k=1}^N \gamma (S_{1,k}^{-1})^2 \chi_{L,k} \left\{ [1 - f_{L,k}] \left[\tilde{\eta}_k \rho \tilde{\eta}_k^\dagger - \frac{1}{2} \{ \tilde{\eta}_k^\dagger \tilde{\eta}_k, \rho \} \right] \right. \\ & \left. + f_{L,k} \left[\tilde{\eta}_k^\dagger \rho \tilde{\eta}_k - \frac{1}{2} \{ \tilde{\eta}_k \tilde{\eta}_k^\dagger, \rho \} \right] \right\}, \quad (12) \end{aligned}$$

and for the site coupled to the right reservoir

$$\begin{aligned} \mathcal{D}_R(\rho) = & \sum_{k=1}^N \gamma (S_{N,k}^{-1})^2 \chi_{R,k} \left\{ [1 - f_{R,k}] \right. \\ & \times \left[\tilde{\eta}_k e^{i\pi\mathcal{N}} \rho e^{i\pi\mathcal{N}} \tilde{\eta}_k^\dagger - \frac{1}{2} \{ \tilde{\eta}_k^\dagger \tilde{\eta}_k, \rho \} \right] \\ & \left. + f_{R,k} \left[\tilde{\eta}_k^\dagger e^{i\pi\mathcal{N}} \rho e^{i\pi\mathcal{N}} \tilde{\eta}_k - \frac{1}{2} \{ \tilde{\eta}_k \tilde{\eta}_k^\dagger, \rho \} \right] \right\}, \quad (13) \end{aligned}$$

where $\chi_{k,L(R)}$ is a temperature-dependent function, $f_{k,L(R)}$ is the Fermi-Dirac distribution,

$$\begin{aligned} f_{L(R),k} &= \frac{1}{e^{\epsilon_k/T_{L(R)}} + 1} \\ \chi_{L(R),k} &= \coth\left(\frac{|\epsilon_k|}{2T_{L(R)}}\right), \quad (14) \end{aligned}$$

and \mathcal{N} is the total number of fermions:

$$\mathcal{N} = \sum_{i=1}^N \tilde{\eta}_i^\dagger \tilde{\eta}_i.$$

The expression for the dissipators can be written in a more elegant form given by

$$\begin{aligned} D_k^L &= A_L^k [\tilde{\eta}_k \rho \tilde{\eta}_k^\dagger - \frac{1}{2} \{ \tilde{\eta}_k^\dagger \tilde{\eta}, \rho \}] + B_L^k [\tilde{\eta}_k^\dagger \rho \tilde{\eta}_k - \frac{1}{2} \{ \tilde{\eta}_k \tilde{\eta}_k^\dagger, \rho \}], \\ D_k^R &= A_R^k [\tilde{\eta}_k e^{i\pi\mathcal{N}} \rho e^{i\pi\mathcal{N}} \tilde{\eta}_k^\dagger - \frac{1}{2} \{ \tilde{\eta}_k^\dagger \tilde{\eta}, \rho \}] \\ &+ B_R^k [\tilde{\eta}_k^\dagger e^{i\pi\mathcal{N}} \rho e^{i\pi\mathcal{N}} \tilde{\eta}_k - \frac{1}{2} \{ \tilde{\eta}_k \tilde{\eta}_k^\dagger, \rho \}], \end{aligned}$$

where we define

$$\begin{aligned} A_L^k &= \gamma (g_{Lk})^2 \chi_{L,k} (1 - f_{L,k}) & B_L^k &= \gamma (g_{Lk})^2 \chi_{L,k} f_{L,k}, \\ A_R^k &= \gamma (g_{Rk})^2 \chi_{R,k} (1 - f_{R,k}) & B_L^k &= \gamma (g_{Rk})^2 \chi_{R,k} f_{R,k}. \quad (15) \end{aligned}$$

Our system is driven out of equilibrium by thermal reservoirs and every site is subjected to dephasing noise. The time evolution of the density matrix is described via a Lindblad master equation with the new dephasing dissipator

$$\mathcal{D}_i^{\text{deph}}(\rho) = \frac{\Gamma}{2} (\sigma_i^z \rho \sigma_i^z - \rho), \quad (16)$$

where Γ is the dephasing strength.

In the presence of dephasing, the Lindblad equation is given by the following representation,

$$\frac{d}{dt} \rho = -i[H, \rho] + \sum_{r=L,R} \mathcal{D}_r(\rho) + \sum_i \mathcal{D}_i^{\text{deph}}(\rho), \quad (17)$$

where $\mathcal{D}_r(\rho)$ are the dissipators given by Eqs. (12) and (13).

In the literature, we have examples that demonstrate interesting effects of the system in the presence of dephasing, specifically the influence on current. As important examples of systems subjected to dephasing noise, we cite Refs. [21,22], which showed the change of the transport regime in the thermodynamic limit with any nonzero dephasing strength, and Ref. [23], which show that the existence of quasiperiodic potentials lead to an enhancement of transport, increasing the system's conductivity.

A. Nonequilibrium steady-state (NESS) equation for the covariance matrix

The fermionic nature of the model allows us to focus on the steady-state properties only on the system's covariance matrix defined as

$$C_{ij} = \langle \eta_j^\dagger \eta_i \rangle, \quad (18)$$

From Eq. (17), we can write the following time evolution for the operator $\langle \eta_n^\dagger \eta_m \rangle$:

$$\begin{aligned} \frac{d}{dt} \langle \eta_n^\dagger \eta_m \rangle &= i \langle [\mathcal{H}, \eta_n^\dagger \eta_m] \rangle + \text{Tr} \{ \eta_n^\dagger \eta_m \mathcal{D}^L \} \\ &+ \text{Tr} \{ \eta_n^\dagger \eta_m \mathcal{D}^R \} + \sum_i \text{Tr} \{ \eta_n^\dagger \eta_m \mathcal{D}_i^{\text{deph}} \}. \quad (19) \end{aligned}$$

Note that the covariance matrix in Eq. (18) is given in terms of the fermionic operators η (η^\dagger) and the dissipators in Eqs. (12) and (13) are given in terms of the new set of fermionic operators $\tilde{\eta}$ ($\tilde{\eta}^\dagger$).

The time evolution for the covariance matrix is

$$\frac{d}{dt} C = -[WC + CW^\dagger] + F - \Gamma \Delta(C), \quad (20)$$

where W and F are temperature-dependent matrices given by $W = iH + S^{-1}MS$:

$$\begin{aligned} \mathcal{M} &= \frac{1}{2} \text{diag}(A_1^L + A_1^R + B_1^L + B_1^R, \dots), \\ \mathcal{B} &= \text{diag}(B_1^L + B_1^R, B_2^L + B_2^R, \dots), \\ F &= SBS^{-1}. \end{aligned}$$

In Eq. (20), $\Delta(C)$ is an operation that removes the diagonal elements of a matrix:

$$\Delta(C) = C - \text{diag}(C_{11}, C_{22}, \dots, C_{NN}). \quad (21)$$

In the NESS, $dC/dt = 0$, which give us the matrix equation

$$WC + CW^\dagger + \Gamma \Delta(C) = F. \quad (22)$$

Note that when $\Gamma = 0$, this reduces to a Lyapunov equation:

$$WC + CW^\dagger = F. \quad (23)$$

Due to the nature of matrices \mathcal{M} and \mathcal{B} , we are able to solve systems up to $N = 100$. When $\Gamma \neq 0$, Eq. (21) is still linear in C , but not in Lyapunov form, and the complexity of the matrix remains the same (we need the eigenvalues and eigenvector of H to solve the system).

III. TRANSPORT PROPERTIES WITH DEPHASING

The classification of the transport regime can be characterized, in general, as a power-law scaling with the system size

$$J \propto \frac{1}{N^\alpha}, \quad (24)$$

where $\alpha \geq 0$ is a transport coefficient. The transport is classified as ballistic, diffusive, and anomalous, which correspond to $\alpha = 0$, $\alpha = 1$, and $\alpha > 1$ or $\alpha < 1$ respectively. In the literature, we have many works devoted to study the behavior

of the current in the presence of dephasing bulk in boundary-driven systems. For a recent review, see Ref. [3].

In this context, our focus here is to go beyond boundary-driven systems and study the behavior of the spin current in the presence of dephasing and thermal baths to induce the system out of the equilibrium.

A. Spin and particle current

Using Eq. (19), we can derive an expression for the particle currents. In the fermionic representation, the temperature imbalance between the two baths will lead to a flow of particles along the chain. In the spin representation, this is mapped into a flow of magnetization.

To evaluate the current of particles and magnetization, we start with a conservation law for the time evolution of $\langle \mathcal{N} \rangle$, where \mathcal{N} is the total number of fermions:

$$\mathcal{N} = \sum_{i=1}^N \tilde{\eta}_i^\dagger \tilde{\eta}_i.$$

Since $[H, \mathcal{N}] = 0$, it follows from Eq. (19) that

$$\begin{aligned} \frac{d}{dt} \langle \mathcal{N} \rangle &= \frac{d}{dt} \text{Tr}\{\mathcal{N}\rho\} \\ &= \text{Tr}\{\mathcal{N}\mathcal{D}_L(\rho)\} + \text{Tr}\{\mathcal{N}\mathcal{D}_R(\rho)\} + \text{Tr}\{\mathcal{N}\mathcal{D}^{\text{deph}}(\rho)\}. \end{aligned} \quad (25)$$

Note that the dephasing dissipator is given by the fermionic operators, and then using the relation between η and $\tilde{\eta}$ (10), we can compute the contribution of $\text{Tr}\{\mathcal{N}\mathcal{D}_i^{\text{deph}}\}$. Using some properties of the fermionic operators, it is easy to show that $\text{Tr}\{\mathcal{N}\mathcal{D}_i^{\text{deph}}\} = 0$, then the dephasing term does not affect the continuity equation. Hence, in NESS we have

$$\begin{aligned} J_{\mathcal{N}} &= \text{Tr}\{\mathcal{N}\mathcal{D}_L(\rho)\} = -\text{Tr}\{\mathcal{N}\mathcal{D}_R(\rho)\} \\ &= \sum_k \gamma g_{L,k} \chi_{L,k} [f_{L,k} - \langle \tilde{\eta}_k^\dagger \tilde{\eta}_k \rangle]. \end{aligned} \quad (26)$$

Defining $\tilde{C}_{ij} = \langle \tilde{\eta}_j^\dagger \tilde{\eta}_i \rangle$ and using Eq. (10), we find

$$\tilde{C}_{ij} = \langle \tilde{\eta}_j^\dagger \tilde{\eta}_i \rangle = \sum_{kl} S_{ik} C_{kl} S_{lj}^{-1} = (SCS^{-1})_{ij}, \quad (27)$$

and then the covariance matrix in the momentum representation is given by $\tilde{C} = SCS^{-1}$, where S is given in terms of the eigenvectors of H . With this result, we can write the particle current as

$$J_{\mathcal{N}} = \sum_k \gamma g_{L,k} \chi_{L,k} [f_{L,k} - \tilde{C}_{k,k}]. \quad (28)$$

This expression is more general and we can use it even when including the dephasing perturbation in Eq. (22).

IV. NUMERICAL ANALYSIS

A. Spin current in homogeneous chain

To better understand the interplay between dephasing and the structure of the Hamiltonian, we study the behavior of a homogenous chain subject to dephasing noise. The Hamiltonian is described by the following interactions:

$$W_{ii} = 2, \quad W_{i+1,i} = W_{i,i+1} = 1; \quad (29)$$

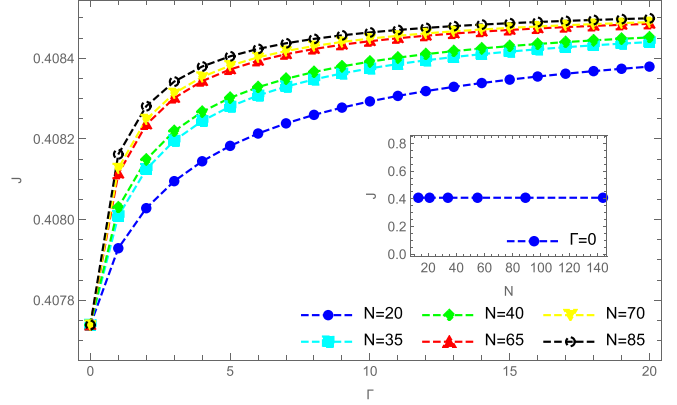


FIG. 1. Spin current as a function of the dephasing strength Γ for different values of N . The temperature gradient is fixed at $\Delta T = 45$ ($T_L > T_R$). We see that the forward current has a small enhancement (less than 1%) even in strong dephasing rate.

that is, we have a homogeneous magnetic field $h_i = 2$ and homogeneous interactions $\alpha_i = 1$. The spin current is depicted in Fig. 1.

When dephasing is present, we have a small enhancement of current (less than 1%) and the ballistic behavior is preserved. As we will see in the next section, the interplay between the graded structure of the Hamiltonian and the dephasing strength raises nontrivial phenomena. Note that this increase of less than 1% is not dependent on N being even or odd.

B. Dephasing enhanced rectification

Now we consider the first case of our numerical analysis. The Hamiltonian is graded and described by

$$h_i = 1, \quad \alpha_i = N - \left(\frac{i-1}{N-1} \right) N + 1; \quad (30)$$

that is, the magnetic field is homogeneous and the spin interaction is decreasing linearly from site 1 to N . We can write

$$H = \sum_{n,m} W_{n,m} \eta_n^\dagger \eta_m, \quad (31)$$

with $W_{n,m}$ given by entries $W_{j,j} = 1$ and $W_{j,j+1} = W_{j+1,j} = \alpha_j$.

For the system to present the rectification phenomenon, it is essential that it presents asymmetry in the interaction between the spins. As soon as we invert the thermal baths, we see different flows. As we discussed in the introduction, it is possible to build devices where we can efficiently handle the magnitude of the current. Specifically, if the left-right symmetry is broken, the magnitude of the spin current, which is given by $J(\Delta T)$ and induced by a positive bias, may be different with respect to the magnitude of $J(-\Delta T)$. We define the rectification factor R as

$$R = \frac{J(\Delta T) + J(-\Delta T)}{J(\Delta T) - J(-\Delta T)}, \quad (32)$$

for $\Delta T > 0$ we have $J(\Delta T) > 0$ [then $J(-\Delta T) < 0$]. This definition is important to see the efficiency of rectification.

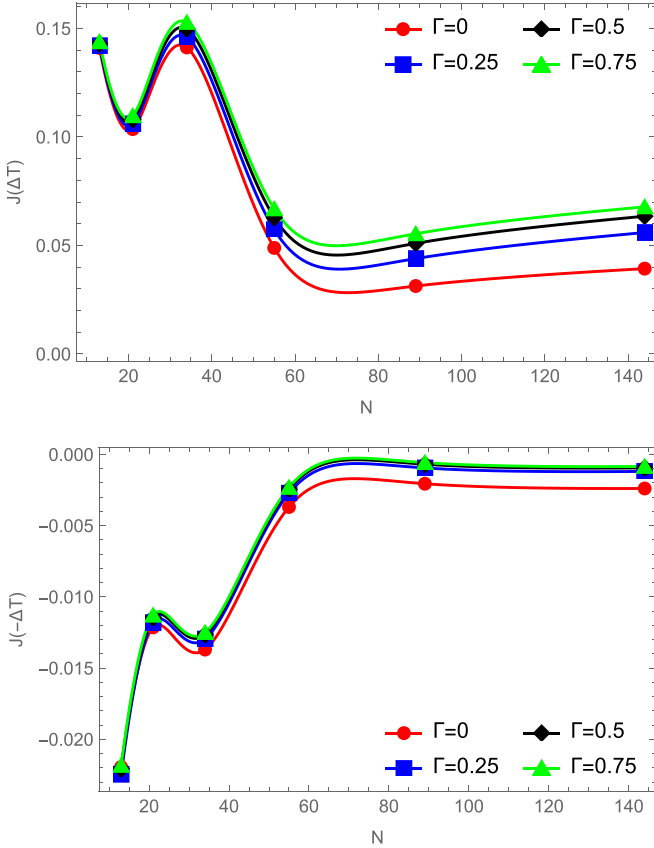


FIG. 2. Spin current for different values of dephasing. The temperature gradient is fixed at $\Delta T = 95$ ($T_L > T_R$) and $h_i = 1$. We see that the forward current is enhanced and the backward current is erased when we increase the dephasing rate.

$R = 0$ means that no rectification takes place [$J(\Delta T) = J(-\Delta T)$], while $|R| = 1$ means that we have perfect rectification (i.e., the current is finite in one direction and null in the other). Other values of R , positive (negative) indicate that the flow is greater for positive (negative) temperature biases. We use the size of the chain following a Fibonacci sequence.

According to Eq. (28), we find the pattern for the spin current shown in Fig. 2.

We see that when dephasing is present the forward current is enhanced (top figure) and the backward current ($\Delta T < 0$) is suppressed (bottom figure) for values of dephasing in $0 < \Gamma < 1$ (Fig. 2) and approaches the curve $\Gamma = 1$ for values of dephasing $\Gamma > 10$ (Fig. 4). Then we get a rectification enhanced phenomenon, depicted in Figs. 3 and 5. We also see that in a limiting case where we have intense dephasing rate, the rectification factor converges to finite values. The decreasing of the rectification factor when N becomes very large is a well-known behavior for systems subject to first neighbor interactions. Even in classical systems of oscillators we have this behavior, but for long-range interactions the rectification factor does not vanish and this phenomenon is due to the new ways of the energy transport which appear and favor the current.

In order to understand the behavior of rectification at large dephasing rate, we plot the same previous figures to compare with this scenario in Fig. 4.

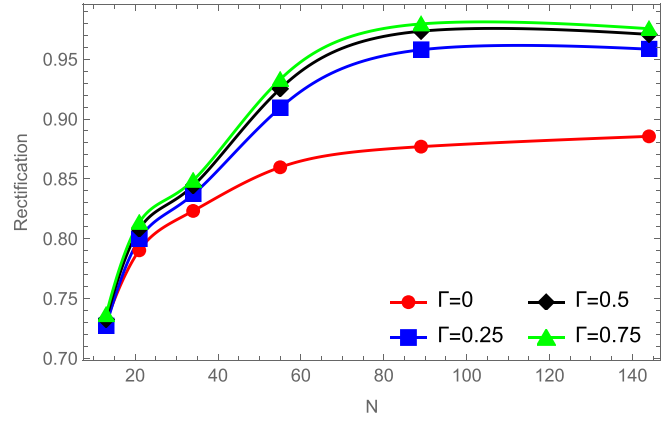


FIG. 3. Rectification pattern of a graded chain described by Eq. (30) for different values of dephasing. The temperature gradient is set at $\Delta T = 95$ ($T_L > T_R$) and $h_i = 1$. When we let the dephasing rate assume more intense values, the rectification is enhanced.

Note that in the presence of dephasing, the rectification factor is not monotonic with N . We also study the behavior of currents in the presence of strong magnetic field, that is,

$$h_i = 8, \quad \alpha_i = N - \left(\frac{i-1}{N-1}\right)N, \quad (33)$$

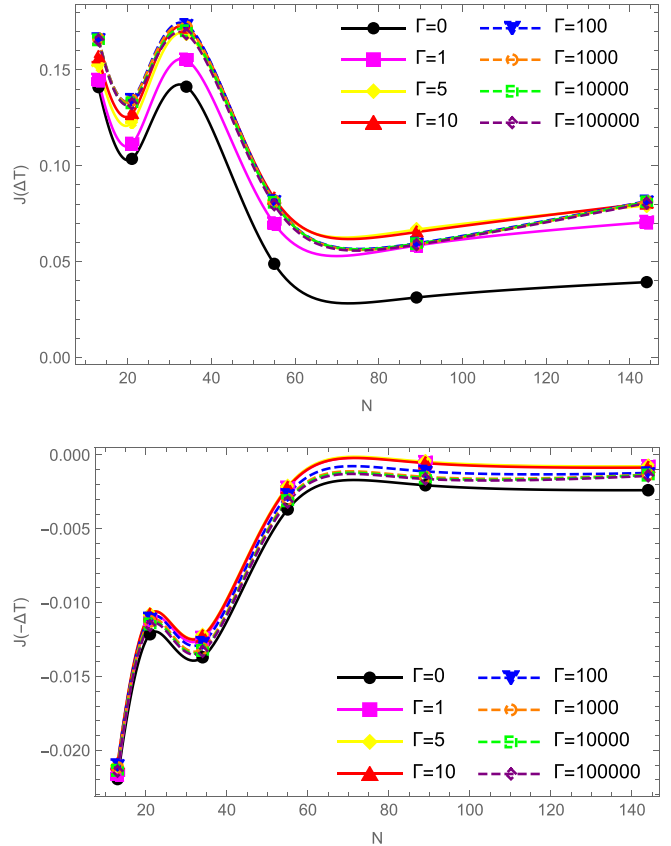


FIG. 4. Spin current for different values of strong dephasing rate. The temperature gradient is fixed at $\Delta T = 95$ ($T_L > T_R$) and $h_i = 1$. We see that the forward current is enhanced and the backward current is erased for dephasing rate less than $\Gamma < 10$ and approaches curve of $\Gamma = 0$ when we increase the dephasing rate above 10.

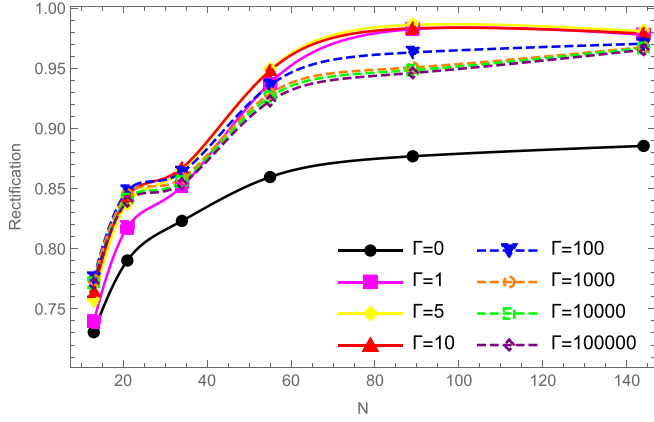


FIG. 5. Rectification pattern of a graded chain described by Eq. (30) for different values of dephasing. The temperature gradient is set at $\Delta T = 95$ ($T_L > T_R$) and $h_i = 1$. When we let the dephasing rate assume more intense values, the rectification is enhanced and for values of dephasing around 10 we have the most intense rectification.

and again we find that, when dephasing is present, the forward current is enhanced and the backward current ($\Delta T < 0$) is erased (Figs. 6 and 7). Then we get a rectification enhanced phenomenon assuming a value closer to one when the magnetic field is stronger (Fig. 8).

Now we investigate the regime of strong magnetic field and also strong dephasing rate. We plot this in Figs. 9–12. Note that for very intense dephasing, the forward current becomes more intense for values of dephasing greater than $\Gamma > 10$ and $N > 50$ (Fig. 9). We see that the existence of the enhancement of the spin rectification does not depend on the strength of the magnetic field. We also observe that we have a saturation of the rectification factor for intense dephasing rate (Fig. 11).

We see that the oscillation behavior dependent on N comes from the graded structure of the system and the small size of N . Also, we believe that this behavior vanishes for larger systems.

It is worth recalling that to compute the heat current and also the spin current we must diagonalize and keep the eigen-

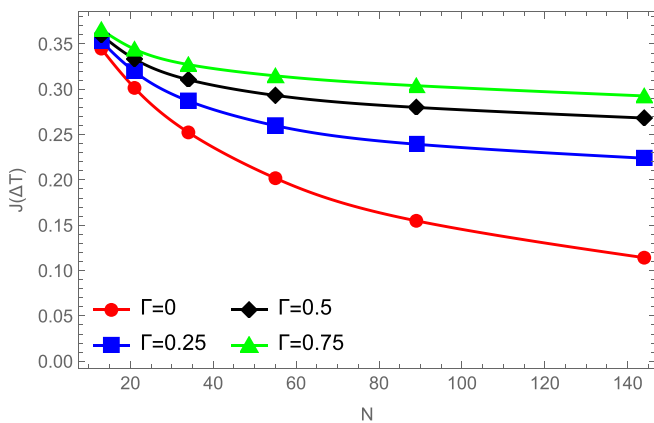


FIG. 6. Forward spin current for different values of dephasing with intense magnetic field. The temperature gradient is fixed at $\Delta T = 95$ ($T_L > T_R$) and the magnetic field is fixed in $h_i = 8$. Again we see that the forward current is enhanced when we grow the dephasing rate.

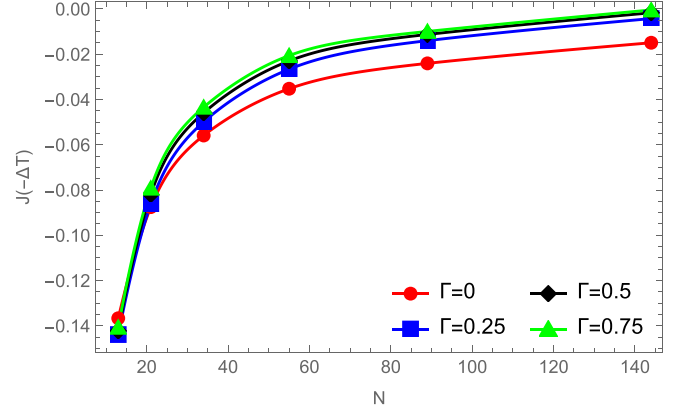


FIG. 7. Backward spin current for different values of dephasing with intense magnetic field ($h_i = 8$). The temperature gradient is fixed at $\Delta T = -95$ ($T_R > T_L$). Again we see that the backward current is essentially erased when we grow the dephasing rate in the region $0 < \Gamma \leq 1$.

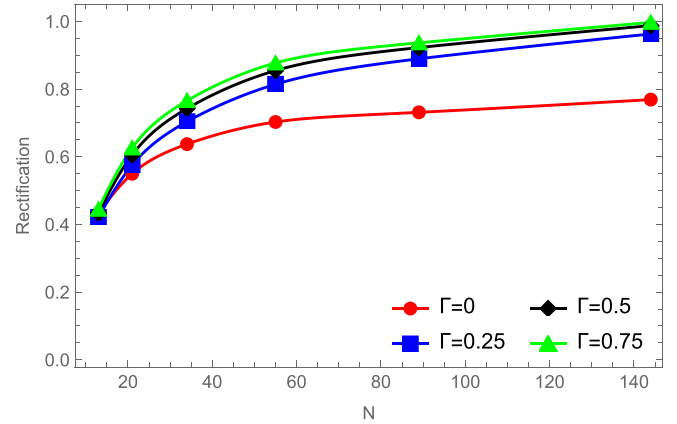


FIG. 8. Rectification pattern of a graded chain described by Eq. (33) for different values of dephasing. The temperature gradient is set at $\Delta T = 95$ ($T_L > T_R$). We let the dephasing rate assume values in $0 < \Gamma < 1$ for strong magnetic field ($h_i = 8$).

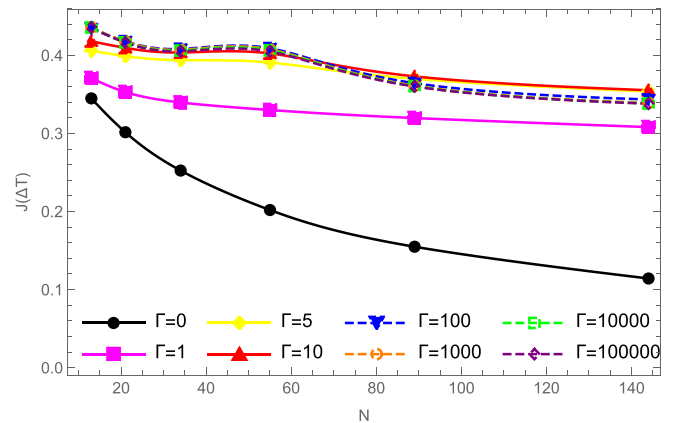


FIG. 9. Forward spin current for different values of dephasing with intense magnetic field. The temperature gradient is fixed at $\Delta T = 95$ ($T_L > T_R$) and the magnetic field is fixed at $h_i = 8$. Again we see that the forward current is enhanced when we increase the dephasing rate, and it essentially saturates for $\Gamma > 10$.

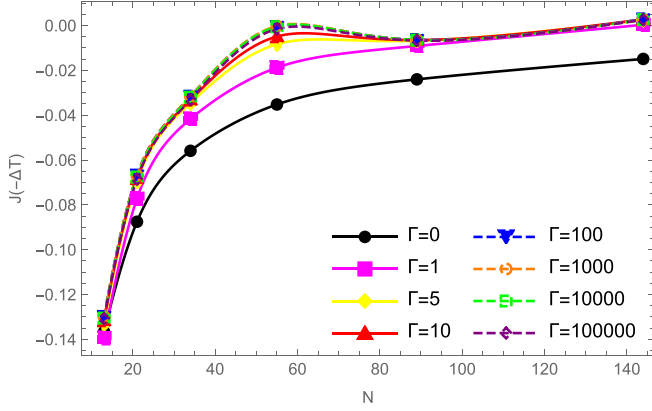


FIG. 10. Backward spin current for different values of dephasing with intense magnetic field ($h_i = 8$). The temperature gradient is fixed at $\Delta T = -95$ ($T_R > T_L$). Again we see that the backward current is erased when we grow the dephasing rate in the region $\Gamma > 10$.

decomposition to perform further calculations, and thus the use of the memory grows when we grow the size of the chain. Here we show even in a regime of strong dephasing rate, we have an enhancement of the rectification of the spin current and also we have the finite value for the rectification factor (Figs. 1–11). Note that for N around 55 and for dephasing rate (Γ) around 10 we have the most significant changes in the data that we presented. Especially in Figs. 5 and 9 we see that there is a maximum near $\Gamma = 10$. This behavior is very interesting and may be due to the size of the chain following a Fibonacci sequence and also the asymmetries caused by the presence of dephasing in the transport phenomena.

C. One-way street of spin current

Now we focus on a fully graded system given by

$$h_i = 1 + \left(\frac{i-1}{N-1}\right)N, \quad \alpha_i = N - \left(\frac{i-1}{N-1}\right)N, \quad (34)$$

that is, the Hamiltonian is composed by a graded magnetic field growing linearly from site 1 to N , and with spin

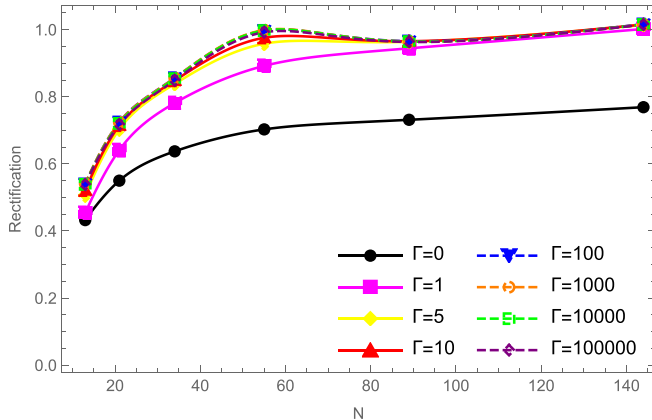


FIG. 11. Rectification pattern of a graded chain described by Eq. (33) for different values of dephasing. The temperature gradient is set at $\Delta T = 95$ ($T_L > T_R$) and $h_i = 8$.

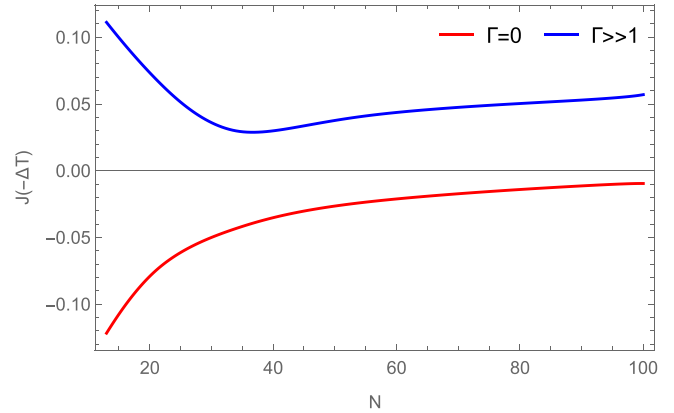
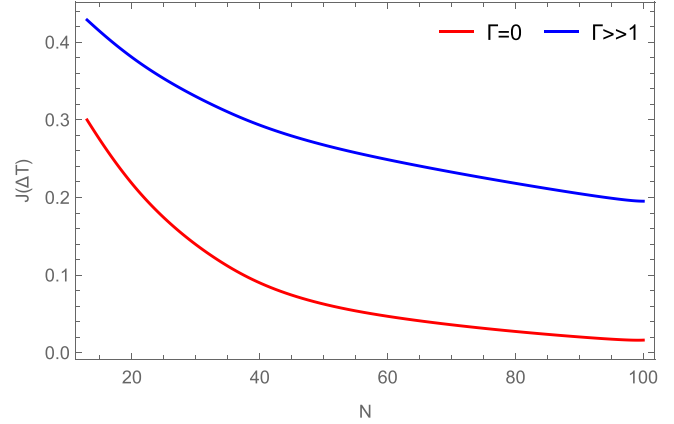


FIG. 12. Spin current for zero dephasing and strong dephasing rate. The temperature gradient is set at $\Delta T = 95$ ($T_L > T_R$). The one way phenomenon (bottom figure) occurs depending on N , ΔT , and Γ .

interaction decreasing linearly from site 1 to N . In this situation, we introduce more asymmetry in the system, and then the interplay between the Hamiltonian and the dephasing term becomes more complex to analyze; that is, with a graded system the coherences are affected.

Using the expression for the spin current in Eq. (28) we find the pattern depicted in Fig. 7. We see that when dephasing is present, the inverse spin current (when the temperature gradient is inverted) assumes a positive value. This phenomenon is dependent on three parameters: the size of the chain (N), the intensity of the dephasing rate (Γ), and the temperature gradient (ΔT).

It is interesting to mention that the one-way phenomenon is due to the symmetry in the expression of the current in the Lindblad equation [32] and it has already been observed in other systems. As an example, we cite the one-way street phenomenon for the energy current in the XXZ model submitted to spin reservoirs at the ends [11]. Here we showed that we have a one-way street also for the spin current in the presence of dephasing noise.

V. FINAL REMARKS

In the present paper, to understand effective mechanisms to manipulate and control currents in quantum systems, we

investigate in detail the spin current in the XX chain subject to graded and nearest neighbor interactions and global dissipators. We derived fully analytical expressions for the computation of heat and spin current. Due the graded structure, the analytical investigation becomes very hard. We recall that the graded structure is necessary to study the phenomenon presented in the paper. For small asymmetry, but not graded, we showed in a previous fully analytical work the existence of thermal rectification on the XX chain, without dephasing [20].

When the system is subject to dephasing noise, we show the existence of nontrivial behavior of spin current; that is, we show the existence of rectification enhancement mechanisms and how it is possible to control the spin current through internal parameters of the microscopic evolution that the system is subjected to (ΔT , N , and Γ). We also observe that it is possible to obtain perfect rectification using graded materials and specific choice of parameters (see Fig. 7). Here, we use thermal baths to induce particle and spin transport, but in a future version we aim to study the behavior of this phenomenon with spin baths and compare it with the thermal baths.

It is also worth recalling that the XX chain has already been shown to be an effective system to obtain rectification [20]. It is interesting to comment that these microscopic systems can be performed experimentally; as an example, we can cite a

more complex system, the XXZ chain, with different values for the coefficients of $\sigma_j^x \sigma_{j+1}^x$, $\sigma_j^y \sigma_{j+1}^y$, and $\sigma_j^z \sigma_{j+1}^z$ [33,34].

Another relevant comment is that the Heisenberg model can be experimentally simulated (implemented). As an example, we mention the study of energy transport by means of cold atoms in optical lattices [35] or trapped ions [36]. Experiments with Rydberg atoms in optical traps involving these spin models are presented in Refs. [37–39].

We reinforce here that for the models that we investigated, the phenomenon presented is difficult to confirm for other graded type of interactions, for example, graded interaction with exponential growth. We also recall that for a classical chain of anharmonic oscillators the rectification factor grows in situations where we have the increasing of the interaction and also in situations with decreasing of the interaction, as presented in Refs. [40].

To conclude, we believe these results aid in the understanding of dephasing effects in the currents of spin chains, and these results will be certainly useful in the problem of manipulation of the currents. Moreover, we believe that the occurrence of rectification in this simple model indicates a ubiquitous phenomenon in spin systems.

ACKNOWLEDGMENT

This work was partially supported by CNPq (Brazil).

-
- [1] S. Lepri, R. Livi, and A. Politi, *Phys. Rep.* **377**, 1 (2003).
 - [2] A. Dhar, *Adv. Phys.* **57**, 457 (2008).
 - [3] G. T. Landi, D. Poletti, and G. Schaller, *Rev. Mod. Phys.* **94**, 045006 (2022).
 - [4] B. Bertini, F. Heidrich-Meisner, C. Karrasch, T. Prosen, R. Steinigeweg, and M. Žnidarič, *Rev. Mod. Phys.* **93**, 025003 (2021).
 - [5] B. Li, L. Wang, and G. Casati, *Phys. Rev. Lett.* **93**, 184301 (2004).
 - [6] N. Li, J. Ren, L. Wang, G. Zhang, P. Hänggi, and B. Li, *Rev. Mod. Phys.* **84**, 1045 (2012).
 - [7] E. Pereira, *Phys. Rev. E* **83**, 031106 (2011).
 - [8] E. Pereira, H. C. F. Lemos, and R. R. Ávila, *Phys. Rev. E* **84**, 061135 (2011).
 - [9] F. Bonetto, J. L. Lebowitz, and J. Lukkarinen, *J. Stat. Phys.* **116**, 783 (2004).
 - [10] F. Barra, *Sci. Rep.* **5**, 14873 (2015).
 - [11] E. Pereira, *Phys. Rev. E* **95**, 030104(R) (2017).
 - [12] J. T. Barreiro, M. Müller, P. Schindler, D. Nigg, T. Monz, M. Chwalla, M. Hennrich, C. F. Roos, P. Zoller, and R. Blatt, *Nature (London)* **470**, 486 (2011).
 - [13] P. Zanardi and L. Campos Venuti, *Phys. Rev. Lett.* **113**, 240406 (2014).
 - [14] S. Diehl, A. Micheli, A. Kantian, B. Kraus, H. P. Büchler, and P. Zoller, *Nat. Phys.* **4**, 878 (2008).
 - [15] V. Popkov, T. Prosen, and L. Zadnik, *Phys. Rev. Lett.* **124**, 160403 (2020).
 - [16] F. Reiter, D. Reeb, and A. S. Sorensen, *Phys. Rev. Lett.* **117**, 040501 (2016).
 - [17] B. Buča, J. Tindall, and D. Jaksch, *Nat. Commun.* **10**, 1730 (2019).
 - [18] T. Werlang, M. A. Marchiori, M. F. Cornelio, and D. Valente, *Phys. Rev. E* **89**, 062109 (2014).
 - [19] E. Pereira, *Phys. Rev. E* **99**, 032116 (2019).
 - [20] S. H. S. Silva, G. T. Landi, R. C. Drumond, and E. Pereira, *Phys. Rev. E* **102**, 062146 (2020).
 - [21] M. Žnidarič, *J. Stat. Mech.* (2010) L05002.
 - [22] A. Asadian, D. Manzano, M. Tiersch, and H. J. Briegel, *Phys. Rev. E* **87**, 012109 (2013).
 - [23] A. M. Lacerda, J. Goold, and G. T. Landi, *Phys. Rev. B* **104**, 174203 (2021).
 - [24] J. J. Mendoza-Arenas, S. Al-Assam, S. R. Clark, and D. Jaksch, *J. Stat. Mech.* (2013) P07007.
 - [25] G. T. Landi, E. Novais, M. J. de Oliveira, and D. Karevski, *Phys. Rev. E* **90**, 042142 (2014).
 - [26] L. Schuab, E. Pereira, and G. T. Landi, *Phys. Rev. E* **94**, 042122 (2016).
 - [27] E. Pereira, *Europhys. Lett.* **126**, 14001 (2019).
 - [28] E. Pereira, *Phys. Lett. A* **374**, 1933 (2010).
 - [29] H. P. Breuer and F. Petruccione, *The Theory of Open Quantum Systems* (Oxford University Press, Oxford, UK, 2002).
 - [30] E. Lieb, T. Schultz, and D. Mattis, *Ann. Phys.* **16**, 407 (1961).
 - [31] E. Lieb, T. Schultz, and D. Mattis, *Rev. Mod. Phys.* **36**, 856 (1964).
 - [32] D. Oliveira, E. Pereira, and H. C. F. Lemos, *Europhys. Lett.* **129**, 10001 (2020).

- [33] M. Endres, H. Bernien, A. Keesling, H. Levine, E. R. Anschuetz, A. Krajenbrink, C. Senko, V. Vuletic, M. Greiner, G. Markus, and M. D. Lukin, *Science* **354**, 1024 (2016).
- [34] D. Barredo, S. De Léséleuc, V. Lienhard, T. Lahaye, and A. Browaeys, *Science* **354**, 1021 (2016).
- [35] I. Bloch, J. Dalibard, and S. Nascimbene, *Nat. Phys.* **8**, 267 (2012).
- [36] R. Blatt and C. F. Roos, *Nat. Phys.* **8**, 277 (2012).
- [37] L.-M. Duan, E. Demler, and M. D. Lukin, *Phys. Rev. Lett.* **91**, 090402 (2003).
- [38] S. Whitlock, A. W. Glaetzle, and P. Hannaford, *J. Phys. B* **50**, 074001 (2017).
- [39] T. L. Nguyen, J. M. Raimond, C. Sayrin, R. Cortiñas, T. Cantat-Moltrecht, F. Assemat, I. Dotsenko, S. Gleyzes, S. Haroche, G. Roux, T. Jolicoeur, and M. Brune, *Phys. Rev. X* **8**, 011032 (2018).
- [40] R. Avila and E. Pereira, *J. Phys. A: Math. Theor.* **46**, 055002 (2013).